Manuscript submitted to: Volume 1, Issue 4, 174-183.

AIMS Materials Science DOI: 10.3934/matersci.2014.4.174

Received date 29 July 2014, Accepted date 14 October 2014, Published date 20 October 2014

Research Article

Preparation of $LiMn_2O_4$ Graphene Hybrid Nanostructure by Combustion Synthesis and Their Electrochemical Properties

Dinesh Rangappa [1,*], Erabhoina Hari Mohan [2], Varma Siddhartha [2], Raghavan Gopalan [2] and Tata Narasinga Rao [2]

[1] Department of Nanotechnology, Center for Post Graduate Studies, Bengaluru Region, VIAT, Muddenahalli, Chikkaballapur-562101 Visvesvaraya Technological University (VTU), Karnataka.

[2] International Advanced Research Centre for Powdered Metallurgy and New Materials (ARCI), Balapur, Hyderabad-500005, India

* **Correspondence:** Email: dinesh.rangappa@vtu.ac.in

Abstract: The $LiMn_2O_4$ graphene hybrid cathode material has been synthesized by spray drying combustion process. The spinel structure cubic phase $LiMn_2O_4$ graphene hybrid material was prepared by spray drying process at 120 °C and subsequent heat treatment at 700 °C for 1 hour. The result indicates that the spinel shaped $LiMn_2O_4$ particles wrapped with graphene sheets were formed with particle size in the range of 60–70 nm. The charge-discharge measurement indicates that the $LiMn_2O_4$ graphene hybrid material shows an improved discharge capacity of 139 mAh/g at 0.1C rate. The pristine $LiMn_2O_4$ nano crystals present only about 132 mAh/g discharge capacity. The $LiMn_2O_4$ graphene hybrid samples show good cyclic performance with only 13% of capacity fading in 30 cycles when compared to the pristine $LiMn_2O_4$ that shows 22% of capacity fading in 30 cycles. The capacity retention of the $LiMn_2O_4$ graphene hybrid samples is about 10% higher than the pristine cycle after 30 cycles.

Keywords: Li ion battery; combustion method; $LiMn_2O_4$; reduced graphene

1. Introduction

Metal oxide based materials have been intensively studied as electrode materials for Lithium ion batteries (LIBs), to achieve higher specific capacities than the traditional electrode materials [1]. Among these, the spinel structure based $LiMn_2O_4$ is considered as one of the potential materials that has replaced the more expensive and toxic layered transition metal oxides such as $LiCoO_2$, $LiNiO_2$, $LiNi_{1/3}Co_{1/3}Mn_{1/3}O_2$ etc. [2–4].

Recently, this has been well marked as one of the cathodes for energy storage system ranging from portable electronic devices to vehicular applications such as EV, HEV, P-HEV's and aerospace application [5]. The $LiMn_2O_4$ is an attractive cathode material for LIB's due to the high voltage, good capacity, abundance of manganese, low cost and environmental benignity. However, this material suffers with poor conductivity and structural instability during charge-discharge process, which is due to the volume expansion and Jahn-Teller distortion [6,7]; dissolution of Mn^{2+} into the electrolyte [8]; and capacity loss [9]. It is highly desirable to overcome these problems to make this $LiMn_2O_4$ meet the requirement of cathode material that is suitable for vehicular application. One way is to dope $LiMn_2O_4$ with different transition metal cations such as Cr, Ni, Al, Co, Fe, Mg, etc. [10,11]. Doping diminishes the dissolution of Mn^{2+} from the $LiMn_2O_4$ structure and suppresses the Jahn-Teller distortion [12]. In addition, partial double doping of two transition metals into the structure will have synergic effect on the cyclability [13].

The $LiMn_2O_4$ compound has been obtained by various methods such as co-precipitation [14], ball milling [15], sol-gel [16], microwave [17], spray pyrolysis [18] and so on. All these methods produce $LiMn_2O_4$ with small particle size. Unfortunately, the nano sized particles prepared by these methods suffer from poor electrical conductivity and strong agglomeration of particles. Sometimes small impurities were also observed, which require high calcinations temperature of about 800 °C to remove those impurities [20,21]. Recently, some researchers deposited the metal oxide on carbon nanotube or reduced graphene oxide to avoid the agglomeration of particles and obtained metal oxide-graphene hybrid electrode [22,23]. Bak et al. prepared $LiMn_2O_4$ reduced graphene hybrid using microwave assisted hydrothermal or solvothermal reaction [24]. Combustion method is another synthesis route that yields finely divided phase pure particles using cheap inorganic reactants (nitrates) and organic fuels (urea, citric acid, glycine, PAA, etc.,) [19,20,21].

In this paper, we report preparation of the $LiMn_2O_4$ graphene hybrid cathode material using modified spray drying combustion processes followed by heat treatment. The spray drying method has advantages of producing homogeneous single crystal nanosize particles. Therefore, combustion and spray drying processes was used for deposition or coating of graphene sheets on the $LiMn_2O_4$. This facilitate have graphene coated nanoparticles. Addition of graphene decreases the dissolution of Mn into the electrolyte and controls volume expansion on charging-discharging process. The porous nature and nanosize of the $LiMn_2O_4$ graphene hybrid shows better electrochemical properties than the pristine $LiMn_2O_4$ sample.

2. Experimental

2.1. Preparation

The stoichiometric amount of raw materials, $LiNO_3$ and $Mn(NO_3).4H_2O$, which act as oxidising agents and sucrose as reducing agent and fuel, were dissolved in minimum amount of DI water. The atomic ratio of Mn/Li is set to be 2:1 and oxidiser to fuel ratio 1:1 [25]. The beaker containing solution was placed on a hot plate at a temperature of 200 °C. After several minutes the combustion process was completed with the evolution of large volumes of gases (N_2, H_2O, CO, NHCO), leaving behind a black powder. The powder was then divided into two parts named hereafter as 1A and 1B. The reduced graphene oxide was prepared by modified Hummer's method [26]. The 1B precursor was mixed with 5 wt% of reduced graphene suspension and spray dried on a hot plate at 120 °C

temperature to obtain $LiMn_2O_4$ graphene hybrid nanocomposite. Then, the obtained 1A and 1B sample powders were ground and calcined initially at 350 °C for 2 hours and then finally at 700 °C in air for 1 hour.

2.2. Characterization

The structure and phase purity of the samples were analysed by Cu-Kά (λ = 1.5418 Aº (in 2θ)) radiation of X-ray diffraction (XRD, Bruker D8-advance, Germany) in the range of 10–70°. The thermal decomposition behaviour of the synthesized nano powder was examined with a thermo-gravimetric analyzer (TG-DSC) on a Netzch (Luxx, sTA, 449, Jupiter, Germany) analyzer under N_2 flow. The TGA spectra were acquired in the temperature range from 30–1000 ºC at a heating rate of 10 ºC min^{-1}. Raman spectra were recorded using Raman spectrometer (Horiba Jobin-Yvon Labtam HR 800) to confirm the formation of $LiMn_2O_4$ graphene hybrid nanocomposite. The morphology and particle size were observed by Field Emission-Scanning Electron Microscopy (FE-SEM; Hitachi's, S-4300 SE/N) and Transmission Electron Microscopy (HR-TEM; Tecnai G-20, 200 KeV) working at 200 KeV.

The electrochemical performance of the samples was investigated by assembling Swagelok cell with Lithium foil as reference and counter electrode. The positive electrodes were prepared from both samples 1 A and 1 B (80 wt%), a mixture of 5 wt% super P carbon and 5 wt% graphite, and polyvinylidene fluoride (PVDF, 10 wt%) was dissolved in N-methyl pyrrolidone. All the components were mixed to form slurry to coat on stainless steel foil current collector and the coated foils were dried in an oven at 100 °C for 12 hours. The electrolyte used was 1M $LiPF_6$ in a mixture of ethylene carbonate (EC) and dimethyl carbonate (DME) with mass ratio of 1:1 and Whattman glass filter paper film was used as separator. The cells were assembled into Swagelok cells within an Argon-filled glove box. Glavanostatic charge-discharge measurement were conducted on an Arbin battery system at different current densities in the voltage range of 3.0–4.5 V (versus Li/Li^+).

3. Results and Discussion

The thermogravimetric curves of $LiMn_2O_4$ graphene hybrid sample prepared by combustion and spray drying before heat treatment is presented in Figure 1. The results show two steps of weight loss, which corresponds to temperature range of 80–150 ºC, and 280–400 ºC. The first weight loss step below 150 ^oC is due to the volatilization of the absorbed water and other organic substances, which corresponds to few endothermic peaks in the DSC curves. The second weight loss between 200–400 ^oC is due to the crystallization of $LiMn_2O_4$ phase and corresponds to exothermic peak in the region 300–400 ^oC [20]. The DSC curves observed are similar to other combustion based $LiMn_2O_4$ sample reported in literature [19,20,21]. The total weight loss during the whole heating process is less than 10%. This indicates that most of the precursor material is converted to amorphous $LiMn_2O_4$ state during the combustion process, which forms crystalline state upon heat treatment.

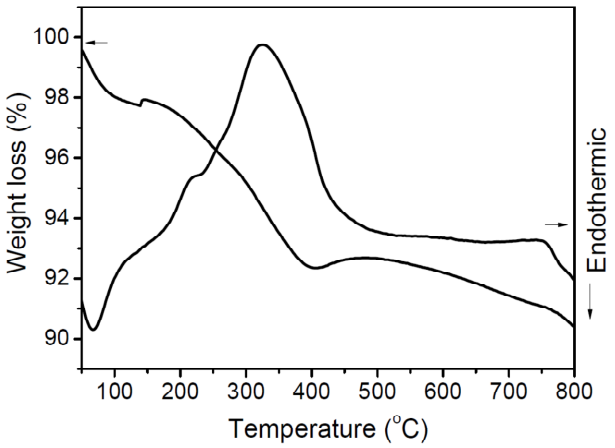

Figure 1. TG-DSC curves of prepared $LiMn_2O_4$-graphene hybrid samples obtained by combustion and spray drying method.

Figure 2 displays the XRD patterns of pristine $LiMn_2O_4$ and $LiMn_2O_4$ graphene hybrid samples obtained by combustion and spray drying followed by heat treatment at 700 °C. The diffraction patterns of both samples are similar. These patterns correspond to a well-defined single phase $LiMn_2O_4$ peaks that can be indexed to cubic spinel structure of Fd3m space group. This is in good accordance with the standard pattern (JCPDS, card no.04-013-6575). The lattice parameters calculated from the diffraction data through the least square program are found to be a = 8.24726 Å and cell volume is 560.96 $Å^3$, which is closest to the standard value reported in literature [27]. For the $LiMn_2O_4$ graphene sample, the characteristic peak of graphene at 2Θ = 26.5 °C was not detected probably due to the small quantity of the graphene used and the strong diffraction signals from the spinel $LiMn_2O_4$ phase. As the crystallinity plays a crucial role on electrochemical performance, a calcination temperature of above 800 °C is considered to be essential for good cyclic performance of the oxide cathode materials [28]. In previous reports, a calcination temperature above 800 ^oC was required to obtain pure $LiMn_2O_4$ phase by solution or combustion based synthesis [19,20,21]. However, in present study, the samples calcined at 700 °C completely transformed into cubic spinel structure of Fd3m space group, in which the Lithium ions occupy the tetrahedral sites (8a), Mn^{3+} and Mn^{4+} ions reside at the octahedral sites (16*d*), and O^{2-} ions are located at 32e sites [29].

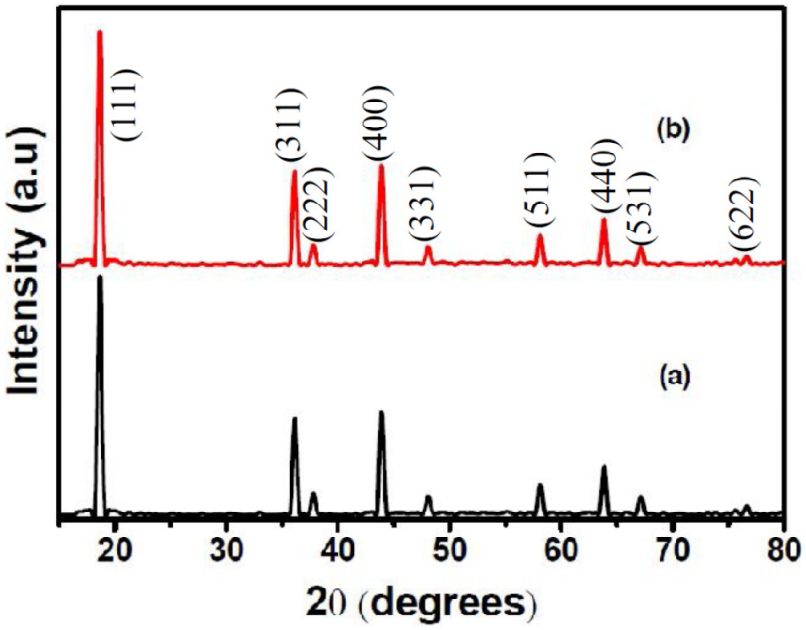

Figure 2. The X-ray diffraction patterns of the (a) pristine $LiMn_2O_4$ and (b) $LiMn_2O_4$-graphene.

The Raman spectra of the both the samples were measured in order to confirm presence of graphene and the formation of $LiMn_2O_4$ graphene hybrid composite and spectra is shown in Figure 3. The presence of a strong band at around 650 cm^{-1} and a group of bands between 200 and 500 cm^{-1} with lower intensity are common features of this spectra. These bands are attributed to the vibrational motion of oxygen atoms inside the octahedral MnO_6 unit [30]. The presence of Mn-O bands confirms that the sample has a spinel structure. The Raman spectrum of $LiMn_2O_4$ graphene sample suggests that the Mn-O bands are marginally shifted to higher frequencies than the pristine $LiMn_2O_4$ nanoparticles. There are two bands observed at around 1336 and 1570 cm^{-1} for $LiMn_2O_4$ graphene sample, which can be attributed to the D-band and G-band of graphene, respectively. The D-band represents the sp^3 structural disorder due mainly to defects in the graphene sheets, whereas G-band reflects the structural integrity of the sp^2-hybridized graphene sheets [31,32].

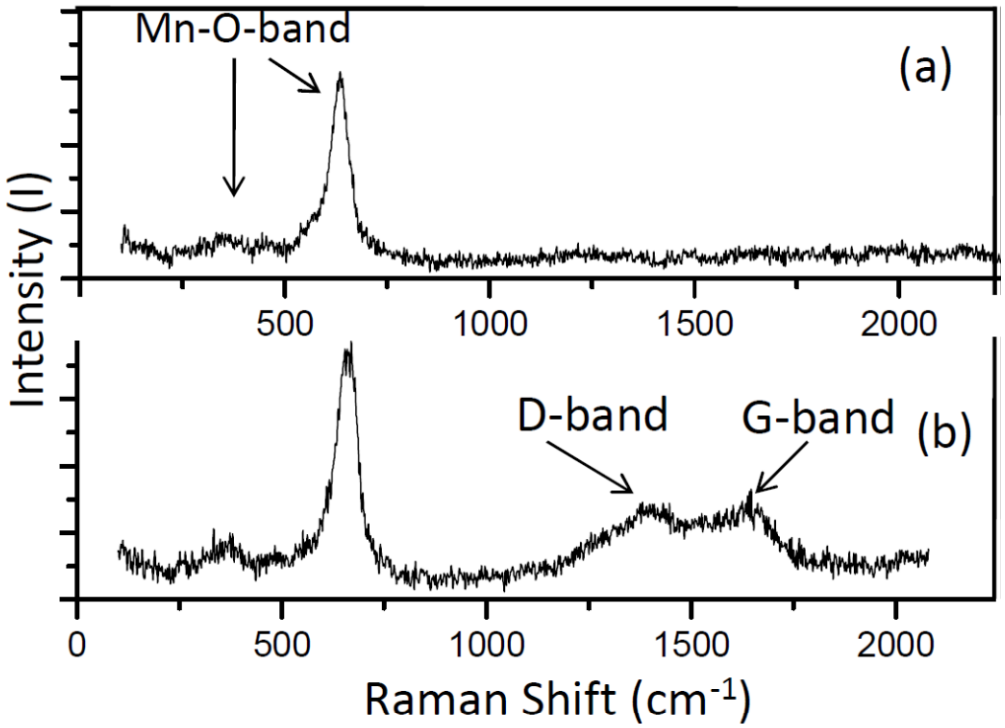

Figure 3. Raman spectra of (a) pristine $LiMn_2O_4$ nanoparticles and (b) $LiMn_2O_4$-graphene sample obtained after heat treatment.

The size and morphology of the heat treated samples were observed using FE-SEM and TEM analysis. It was found that the sample prepared by combustion process shows porous morphology as shown in Figure 4 (a). The typical images of spray dried coated $LiMn_2O_4$-graphene hybrid sample is shown in Figure 4 (b). It can be observed that small $LiMn_2O_4$ particles were coated with graphene sheet. These small particles formed porous agglomerate particles, which is good for Li ion battery application as the electrolyte can be accessed through this porous structure. Figure 4c represents TEM images of pristine $LiMn_2O_4$ particles with size about 60 nm. The images in the Figure 4d and e show the TEM images of $LiMn_2O_4$ graphene samples. Two types of graphene and $LiMn_2O_4$ coating were observed from the TEM images. In Figure 4d, we can observe that $LiMn_2O_4$ nanoparticles were deposited on the surface of graphene sheets, which is indicated by arrow mark. Whereas, in Figure 4e the $LiMn_2O_4$ nanoparticles wrapped up with graphene sheets can be observed. This sample shows hexagonal and bipyramidal shaped particles with size in the range of 50–60 nm. The $LiMn_2O_4$ nanoparticles with small particle size and good graphene coating on the particle surface are suitable for high capacity cathode materials.

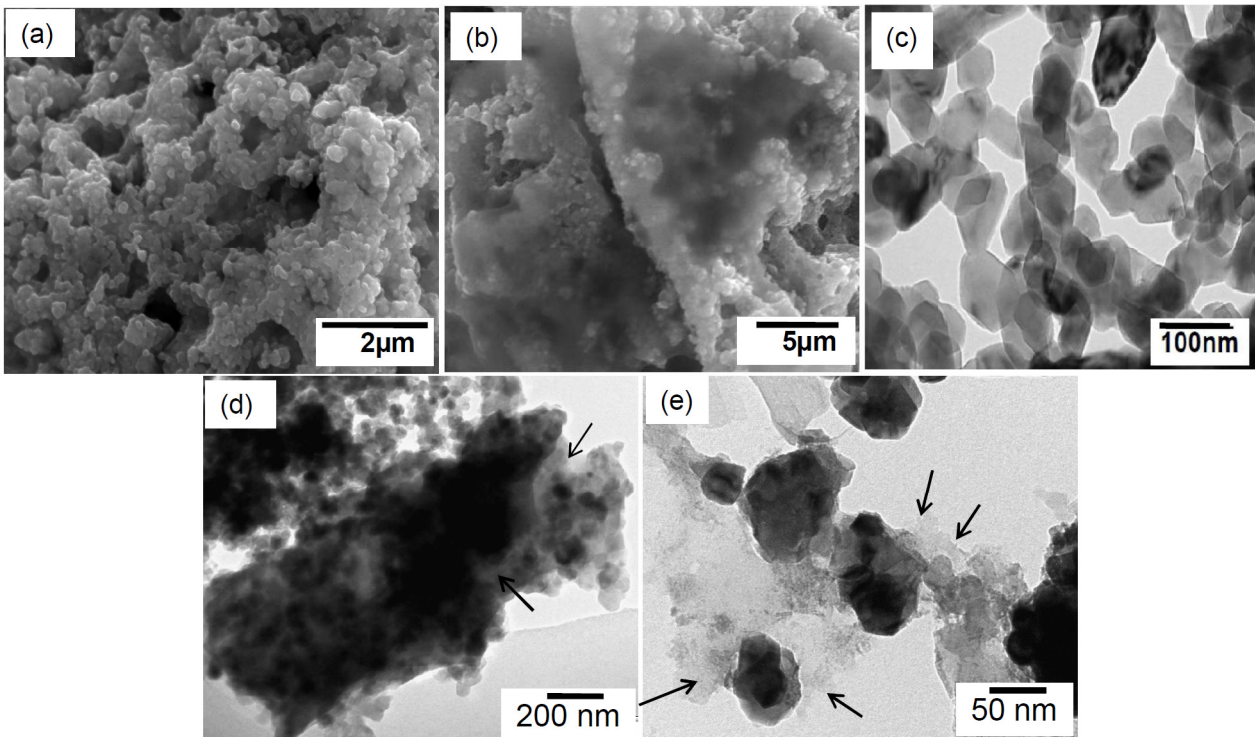

Figure 4. FE-SEM images of (a) pristine $LiMn_2O_4$ and (b) $LiMn_2O_4$-graphene. TEM images of (c) pristine $LiMn_2O_4$ and (d-e) $LiMn_2O_4$-graphene. (d) Shows the $LiMn_2O_4$ nanoparticles deposited on the surface of graphene and (e) shows the $LiMn_2O_4$ nanoparticles wrapped by graphene sheets.

Figure 5a shows the initial charge–discharge profile at room temperature (25 °C) of $LiMn_2O_4$/Li cell, voltage applied between 3.0 and 4.5 V for pristine $LiMn_2O_4$ and $LiMn_2O_4$ graphene. It was observed that two distinct plateaus appeared on the charge curve as well as on the discharge curve for both the cathodes as shown in Figure 5a, respectively. From the charge and discharge curves, it was also observed that graphene coated $LiMn_2O_4$ (1B) had a slightly higher initial discharge capacity (139 mA h/g) than that of pristine $LiMn_2O_4$ (1A) (132 mA h/g) at 0.1C rate. This slight increase in capacity of $LiMn_2O_4$-graphene sample can be attributed to the improved conductivity of the sample due to graphene wrapping on the $LiMn_2O_4$ and the fact that Li^+–Li^+ coulombic repulsion is lower at the surface of nanomaterials enhancing local Li capacity because there is no neighbouring Li^+ outside the particle [33].

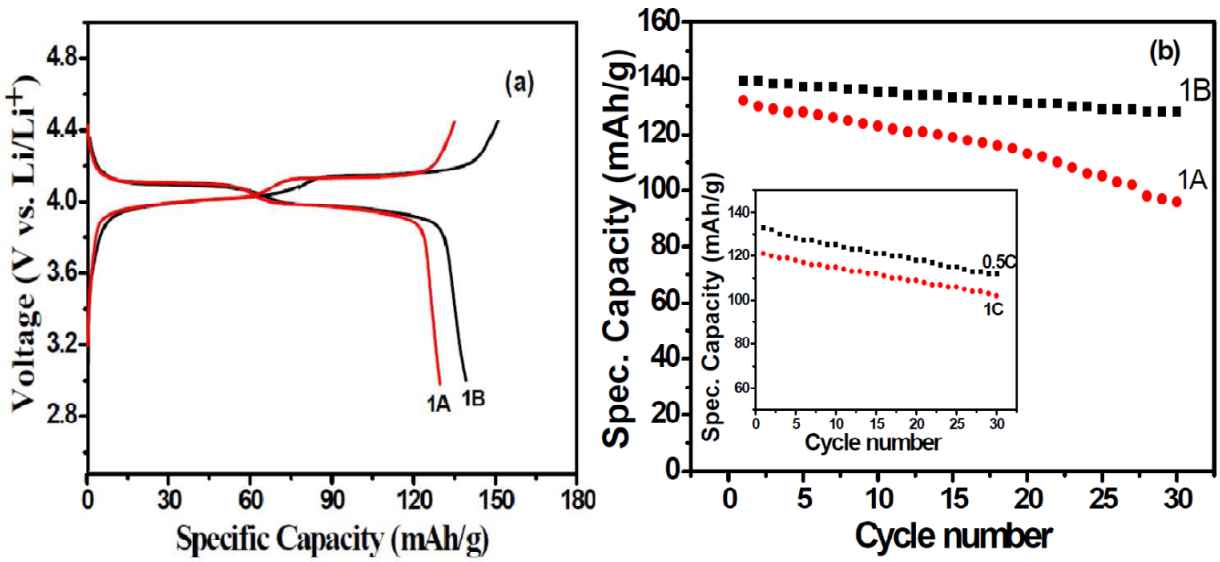

Figure 5. (a) charge-discharge curves of pristine $LiMn_2O_4$ (1A) and $LiMn_2O_4$-graphene (1B) samples; (b) cycle life of pristine $LiMn_2O_4$ (1A) and $LiMn_2O_4$-graphene (1B) at0.1C rate. In set plot shows the cyclic performance of 1B at different C-rates.

Figure 5b shows the discharge capacity vs. the cycle number plots of pristine $LiMn_2O_4$ and $LiMn_2O_4$-graphene cells at room temperature (25 °C) for the first 30 cycles. The $LiMn_2O_4$ graphene cells deliver a discharge capacity of 139, 133 and 121 mAh/g at 0.1, 0.5 and 1 C, respectively, at initial cycle. At the end of 30 cycles the capacity retention is about 87, 85 and 84% at 0.1, 0.5 and at 1 C respectively. The capacity retention of $LiMn_2O_4$ graphene hybrid is about 92% of theoretical capacity at 0.1 C, when compared to pristine samples, which show only 73% after 30 cycles. This indicates that the hybrid sample shows about 20% higher capacity retention that can be attributed to the fact that the $LiMn_2O_4$ nanocrystals are either deposited on the conductive graphene sheets as observed in the Figure 4d or wrapped by graphene sheets as in Figure 4e. The graphene coating on the particle avoids the direct contact of particles with electrolyte, therefore, the dissolution of Mn could be prevented. In addition, it also reduces the Jahn-Teller distortion and decreases the volume expansion. These results are better than the previous reports, where about 30–40% capacity loss was common after the initial discharge cycles [26]. Thus, the $LiMn_2O_4$ graphene hybrid material with high crystallinity shows improved electrochemical cycling performance compared with pristine $LiMn_2O_4$.

4. Conclusion

$LiMn_2O_4$ graphene hybrid cathode has been synthesized by a two-step process. The amorphous $LiMn_2O_4$ obtained by combustion process was spray dried with reduced graphene on hot plate at 120 °C followed by heat treatment at 700 °C for 1 hour. The results reveal that both pristine $LiMn_2O_4$ and $LiMn_2O_4$ graphene samples have well-ordered crystallinity and high phase purity. The FE-SEM and TEM images show that the 60 nm (approx.) sized $LiMn_2O_4$ particles are either deposited on the graphene sheets or wrapped by the same resulting in hybrid material. The $LiMn_2O_4$-graphene sample exhibits a high initial capacity of 139 mAh/g, which is about 94% theoretical capacity at a discharge

rate of 0.1C than that of the pristine $LiMn_2O_4$ (132 mAh/g). It also exhibits good rate capabilities of 133 and 121 mAh/g at 0.5 and 1C, respectively, and show about 20% higher capacity retention in 30 cycles than the pristine sample.

Acknowledgement

The authors acknowledge Dr. Y. Srinivas Rao (Centre for Ceramic, ARCI) and Mr. L. Venkatesh for the TG and DSC and FESEM measurements. Thanks are also due to Akki Bhasker (IIT Hyderabad) for helping in the electrochemical measurement.

References

1. Maclean LAH, Poinsignon C, Amarilla JA, et al. (1995) Electrochemical behaviour of natural and synthetic ramsdellite. *J Mater Chem* 5: 1183–1189.
2. Xia Y, Zhou Y, Yoshio M (1997) Capacity Fading on Cycling of 4 V Li / $LiMn_2O_4$ Cells. *J Electrochem Soc* 144: 2593–2600.
3. Tsai YW, Santhanam R, Hwang BJ, et al. (2003) Structure stabilization of $LiMn_2O_4$ cathode material by bimetal dopants. *J Power Sources* 119: 701.
4. Jeong WT, Joo JH, Lee KS (2003) Improvement of electrode performances of spinel $LiMn_2O_4$ prepared by mechanical alloying and subsequent firing. *J Power Sour* 119: 690–694.
5. Schalkwijk V, Scrosati WA, Eds B (2002) Advances in Lithium-ion Batteries, Kluwer Academic/Plenum Publishers, New York.
6. Wang XL, Feygenson M, Aronson MC, et al. (2010) Sn/SnO_x core-shell nanospheres: Synthesis, anode performance in Li–Ion batteries, and superconductivity. *J Phys Chem C*114: 14697–14703.
7. Thackeray MM, Shao- Horn Y, Kahaian AJ, et al. (1998) Structural Fatigue in Spinel Electrodes in High Voltage (4 V) Li/$LixMnzO_4$ Cells. *Electrochem Solid State lett* 1: 7.
8. Saitoh M, Yoshida S, Yamane H, et al. (2003) Capacity Fading of the Acid-treated Lithium Manganese Oxides in High-temperature Storage. *J Power Sources* 122: 162–168.
9. Shin Y, Manthiram A (2002) Microstrain and Capacity Fade in Spinel. Manganese Oxides. Electrochem *Solid State Lett* 5: A55–A58.
10. Taniguchi I (2005) Powder properties of partially substituted $LiM_xMn_{2-x}O_4$ (M = Al, Cr, Fe and Co) synthesized by ultrasonic spray pyrolysis. *Mater Chem Phys* 92: 172–179.
11. Jeong IS, Kim JU, Gu HB (2001) Electrochemical properties of $LiMgyMn_{2-y}O_4$ spinel phases for rechargeable lithium batteries. *J Power Sources* 102: 55–59.
12. Yi TF, Zhu YR, Zhu XD (2009) A review of recent developments in the surface modification of $LiMn_2O_4$ as cathode material of power lithium-ion battery. *Ionics 15*: 779–784.
13. Amarilla JM, Petrov K, Pico F, et al. (2009) Sucrose-aided combus-tion synthesis of nanosized LiMn1.99·yLiyM0.01O4 (M = Al^{3+}, Ni^{2+}, Cr^{3+}, Co^{3+}, y = 0.01 and 0.06) spinels. *J Power Sources* 191: 591–600.
14. Chan HW, Duh JG, Sheen SR (2003) $LiMn_2O_4$ cathode doped with excess lithium and synthesized by co-precipitation for Li-ion batteries. *J Power Sources* 115: 110–118.
15. Choi HJ, Lee KM, Kim GH (2001) Mechanochemical synthesis and electrochemical properties of $LiMn_2O_4$. *J Am Ceram Soc* 84: 242–244.

16. Sun YK, Oh IH, Kim KY (1997) Synthesis of Spinel $LiMn_2O_4$ by the Sol-Gel Method for a Cathode-Active Material in Lithium Secondary. *Ind Eng Chem Res* 36: 4839–4846.
17. Yan H, Hnang X, Chen L (1999) *J Power Source* 81: 647–650.
18. Ohano K, Saitou M (2003) Techinical Report.
19. Du K, Zhang H (2003) Preparation and performance of spinel $LiMn_2O_4$ by a citrate route with combustion. J Alloy Compd 352: 250–254.
20. Fey GTK, Cho YD, Kumar TP (2006) Mater. Chem. Phys. 99: 451–415.
21. Park HB, Kim J, Lee CW (2001) Synthesis of $LiMn_2O_4$ powder by auto-ignited combustion of poly(acrylic acid)-metal nitrate precursor. *J Power Sources* 92: 124–130.
22. Liu XM, Huang ZD, Oh S, et al. (2010) Sol-gel synthesis of multiwalled carbon nanotube-$LiMn_2O_4$ nanocomposites as cathode materials for Li-ion batteries. *J Power Sources* 195: 4290–4296.
23. Paek SM, Yoo E (2009) I. Honma, Nano Lett, 9: 72–76.
24. Bak SM, Nam KW, Lee CW, et al. (2011) Spinel $LiMn_2O_4$/reduced graphene oxide hybrid for high rate lithium ion batteries. *J Mater Chem* 21: 17309–17315.
25. Jain SR, Adiga KC, Verneker VR (1981) A New Approach to Thermochemical Calculations of Condensed Fuel-Oxidizer Mixtures. *Comb Flam* 40: 71–79.
26. Hummers WS, Offeman RE (1958) Preparation of Graphitic Oxide. *J Am Chem Soc* 80: 1339.
27. Hon YM, Lin SP, Fung KZ, et al. (2002) Synthesis and characterization of nano-$LiMn_2O_4$ powder by tartaricacid gel process. *J Euro Ceram Soc* 22: 653–660.
28. Spakr ME, Novak P, Schnyder B et al. (1998) J Electrochem Soc 145: 1113.
29. Thackeray MM, David WIF, Bruce PG (1983) Lithium Insertion Into Manganese Spinels. *Mater Res Bull* 18: 461–472.
30. Ramana CV, Massot M, Julien CM (2005) XPS and Raman spectroscopic characterization of $LiMn_2O_4$ spinels. *Surf Interface Anal* 37: 412–416.
31. Ma PC, Kim JK, Tang BZ (2006) Functionalization of carbon nanotubes using a silane coupling agent. *Carbon* 44: 3232–3238.
32. Geng Y, Wang SJ, Kim JK (2009) Preparation of graphite nanoplatelets and graphene sheets. *J Colloids Interface Sci* 336: 592–598.
33. Veluchamy A, Ikuta H, Wakihara M (2001) Boron-substituted manganese spinel oxide cathode for lithium ion battery. *Solid State Ionis* 143: 161–171.
34. Sinha NN, Munichandraiah N (2009) The effect of particle size on performance of cathodematerials of Li-ion batteries. *J Library IISc Ernet* 89: 381–392.
35. Wagemaker M, Kearley GJ, Van-Well AA, et al. (2003) Multiple Li positions inside oxygen octahedra in lithiated. TiO_2 anatase. *J Am Chem Soc* 125: 840–848.